Available online at www.sciencedirect.com
ScienceDirect
Geomorphology 93 (2008) 89–103
GEOMORPHOLOGY
www.elsevier.com/locate/geomorph

Comparison of GPR, 2D-resistivity and traditional techniques for the subsurface exploration of the Öschingen landslide, Swabian Alb (Germany)

O. Sass [a,*], R. Bell [b], T. Glade [b]

[a] Institute of Geography, University of Augsburg, Universitätsstr. 10, 86135 Augsburg, Germany
[b] Department of Geography, University of Bonn, Meckenheimer Allee 166, 53227 Bonn, Germany

Received 20 June 2005; accepted 22 December 2006
Available online 25 April 2007

Abstract

Numerous rotational and translational slides of different sizes cause considerable economic damage in the Swabian Alb (SW-Germany) and are a challenge for risk assessment. The Öschingen landslide is a typical example for landslides occurring along the escarpment. Lithology consists of Jurassic sedimentary rocks involving clays overlain by marls and limestones. A combination of traditional methods (drilling, mapping, inclinometers) and geophysical techniques (2D-resistivity (ERT), ground-penetrating radar (GPR)) was applied to gain knowledge about the thickness and internal structure of the landslide.

The drillings and penetration tests provided point information on landslide extent, structure and material involved. In general, all inclinometers showed very little movement if at all. The GPR results were affected by strong signal attenuation and by overhead reflections from the nearby woods. Despite these general obstacles for the application of GPR on landslides near-surface sediment structures were detected. In the 2D-resistivity sections, higher-resistive limestone blocks reaching 10–15 m in thickness could be clearly distinguished from the underlying bedrock. The detailed two-dimensional data of the electrical resistivity tomography (ERT) along with the rather high survey speed turned out to be the best choice to gain detailed spatial information on thickness and extent of the slope movement. The measured profiles coincide with the GPR data and correspond to borehole data.

Surprisingly, all results from the applied methods clearly detected the absence of large landslide blocks in the north-west of the study area. This finding could not be concluded from local geomorphology of this area. Regarding the current landslide displacement derived from the inclinometer measurements, the large landslide blocks seem to be dormant during the measured period.

Keywords: Landslide; Ground-penetrating radar; 2D-resistivity; Swabian Alb

1. Introduction

In the Swabian Alb (SW-Germany), the slopes of the cuesta landscape formed by limestones overlaying marls and clays are very prone to landsliding. Numerous rotational and translational slides of different size and age can be found. The largest landslides are supposed to be either of Pleistocene or Holocene age (Terhorst, 1997; Bibus, 1999; Kallinich, 1999). However, the 1983 Mössingen landslide with 6 million m^3 (Bibus, 1986; Schädel and Stober, 1988) causing 1.5 million €

* Corresponding author. Tel.: +49 821 598 2279.
E-mail address: oliver.sass@geo.uni-augsburg.de (O. Sass).

0169-555X/$ - see front matter © 2007 Elsevier B.V. All rights reserved.
doi:10.1016/j.geomorph.2006.12.019

damage on forest and forest roads (Fundinger, 2006), showed that such large events have the potential to threaten the society even today. In total four events of similar size have occurred in the last 218 years (Kallinich, 1999). Considering that this total number is based purely on historical records and thus, gives minimum frequency of such large events (Glade, 2001), these events should not be neglected in landslide hazard and risk assessment.

Landslides in the Swabian Alb are mainly threatening roads, railways, houses and to a lesser extent people. Until today, only one fatal landslide is known which caused the death of three people in 1960 (Schädel and Stober, 1988). In contrast, economic damage is rather high and commonly includes burying or destruction of roads and railways, as well as damage to buildings and forest. For example, the most recent landslide on the 18 March 2005 blocked the railway line near Biesingen–Steinhofen for some days and caused significant direct, but in particular non-quantified indirect costs through additional bus shuttles and interruption of traffic. The contrast between landslide occurrence throughout the region and rare information on economic damage, historic information and landslide perception led to the establishment of the project *Integrative landslide risk analysis and risk evaluation in the Swabian Alb, Germany (InterRISK)*.

Despite the growing body of general information on landslides, the prediction and risk assessment in a certain area of investigation still requires the assessment of detailed field data (Glade et al., 2005a,b). Besides surface investigations such as mapping, field surveys, etc., the subsurface exploration is of major importance to gain knowledge about the thickness and internal structure of the landslide. This study focuses on the Öschingen landslide which is a typical example for the very widespread landslide occurrences along the escarpment of the Swabian Alb.

In assessing the landslide hazard, it is crucial to examine the structure of the sliding masses (including the depth of shear surfaces) and its movement patterns. Traditional techniques to investigate subsurface structure and landslide dynamics include e.g. drillings, penetration tests and inclinometers for obtaining subsurface movement patterns (e.g. Demoulin and Glade, 2004; Glade et al., 2005a; Marcato et al., 2006). An overview on traditional techniques for subsurface exploration of landslides and field instrumentation is provided by McGuffey et al. (1996), Mikkelsen (1996) and Ortigao (2004).

While it is very expensive and time-consuming to carry out deep drillings in the required narrow mesh, geophysical methods are generally quicker and cheaper and provide highly resolved two-dimensional subsurface information. Although there have been many geophysical investigations on landslides to date, the knowledge about the potency and limitations of various techniques is still incomplete. A wide range of geophysical techniques is at hand to assess the near-subsurface geometry, of which seismic refraction and geoelectrical methods are most widely implemented (e.g. Mauritsch et al., 2000; Hecht, 2001, 2003; Bichler et al., 2004; Glade et al., 2005a).

Due to the generally rather wet and clayey material of landslides, a broad variety of methods using electrical or electromagnetic conductivity have been applied. Many attempts are undertaken to investigate the subsurface structure using vertical electrical sounding (e.g. Mauritsch et al., 2000; Israil and Pachauri, 2003; Agnesi et al., 2005). However, as Bogolovsky and Ogilvy (1977) pointed out, the physical properties within a landslide area can vary greatly over very small distances. This problem is even more critical when unfavourable geometric circumstances like a strongly undulated bedrock surface obstruct the survey (Mauritsch et al., 2000). The lack of lateral resolution is overcome by two-dimensional methods like electrical resistivity tomography (ERT). This method reveals a great heterogeneity of landslide material (e.g. Godio and Bottino, 2001; Wetzel et al., 2006; Bell et al., 2006) and can even be applied on the monitoring of groundwater flow in landslides (Suzuki and Higashi, 2001).

In contrast, ground-penetrating radar as a very highly resolved two-dimensional technique has been rarely used on landslides to date (e.g. Bichler et al., 2004); the possible reasons for that are highlighted in the Methodology section. However, important slip zones in landslide bodies are frequently very thin so that geoelectrical or seismic techniques may not detect them. Thus, it was one of the aims of this research to find out whether GPR can contribute to subsurface information on comparatively high-resistive sliding masses like the supposed limestone blocks in the area of investigation.

The main aim of this study is to obtain information on the lateral and vertical extent of the Öschingen landslide masses within a subarea of the total landslide complex. Secondly, the suitability of various geophysical methods was tested and compared to traditional techniques. The most suitable methods were then selected and used for further detailed studies on the subsurface structure and dynamics of the landslide. Final results will be the basis for slope stability analysis and the preparation of landslide hazard and risk maps.

2. Study area

The Öschingen landslide complex is located in the Central Swabian Alb, SW-Germany (Fig. 1). The study area covers approximately 1.3 km^2. Local topography is determined by the cuesta landscape. Lithology consists of Jurassic sedimentary rocks. The original topography involves flat slopes within the middle Jurassic clays (Callovian, up to 640 m a.s.l.), steeper slopes within the Oxford marls (Ox 1, up to 720 m a.s.l.) and a steep slope within the Oxford limestone (Ox 2), which also builds up the plateau at 800 m a.s.l. On top of the plateau Kimmeridge marls (Ki 1) can be found. In general, slopes are covered with up to 10 m thick debris layer (Terhorst, 1997). The strata dip 3° towards the east (Schmidt, 1994). The average annual temperature is about 9 °C and average rainfall ranges between 800 and 900 mm per year (Bibus, 1986; Kreja and Terhorst, 2006). In addition to intense rainfall events, the study area is prone to earthquakes (Schneider, 1971).

The Öschingen landslide occurred on a spur and its eastern flank. The landslide complex shows different landslide blocks, two to three above each other on the slope. The question whether these blocks belong to successive rotational slides, multiple rotational slides or a single rotational slide remains open (according to the classification of Cruden and Varnes, 1996 and Dikau et al., 1996). Related to this is the question of the time dimension of the failure(s).

Most parts of the landslide complex are covered with dense forest. On gentler footslopes or slope terraces grasslands can be found. Settlement development on the landslide area started in the 1960s and 1970s. Today, some parts of the landslide toe are inhabited (Fig. 2A). Some buildings in this area show damage, which might have resulted from slope movements (Fig. 2B). If the

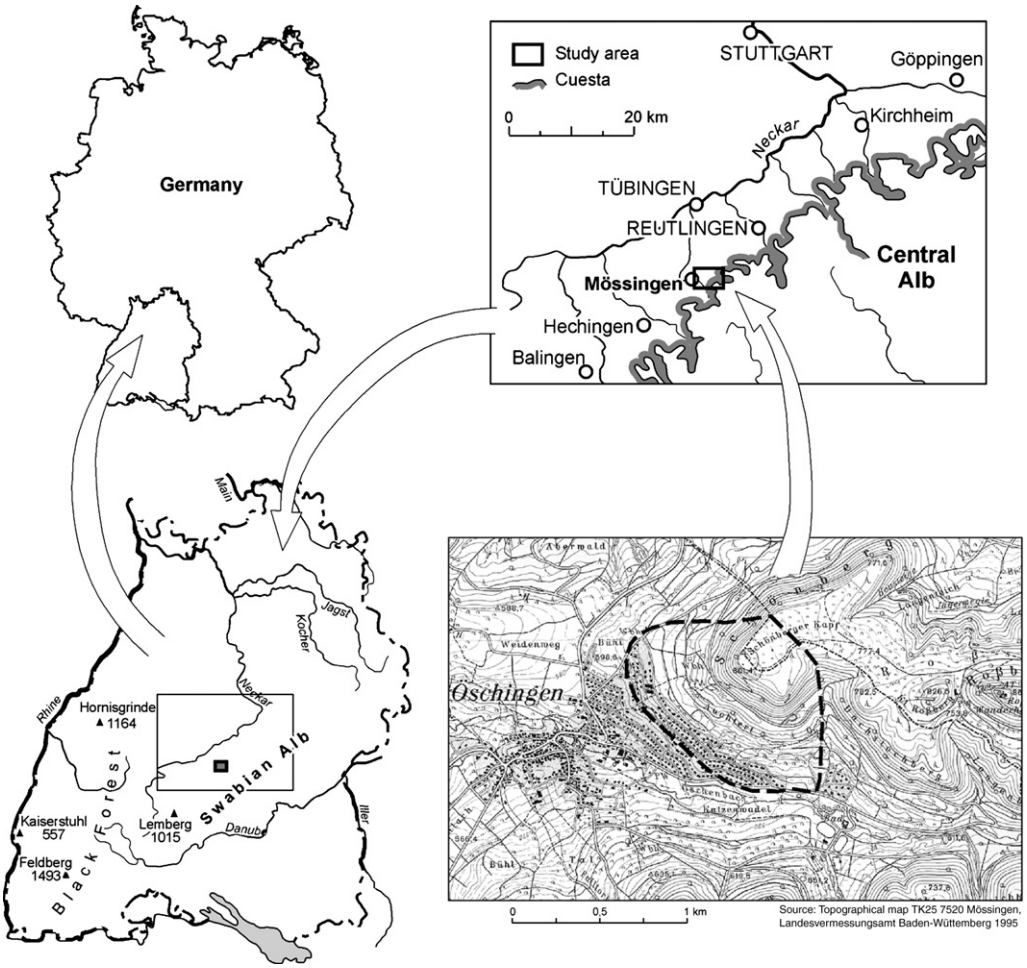

Fig. 1. Location of the study area in Southern Germany.

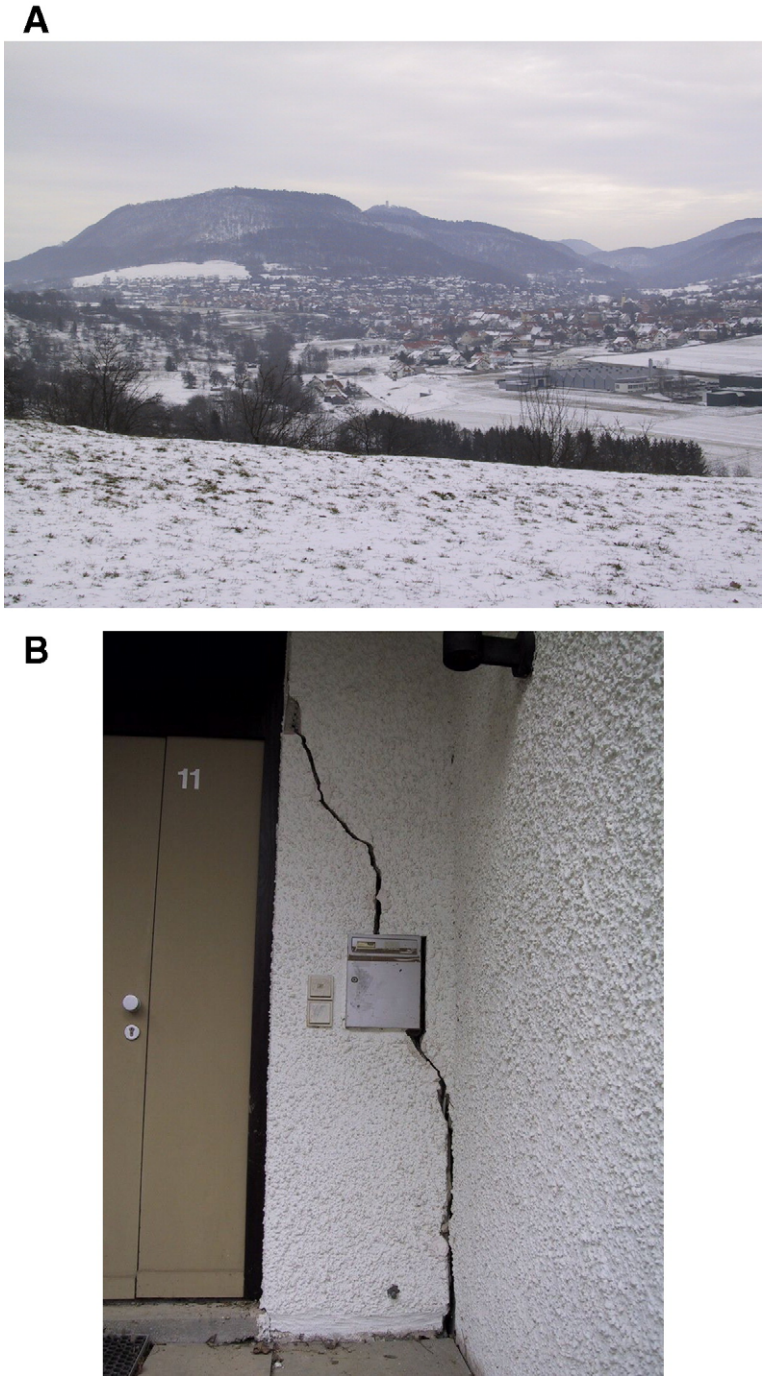

Fig. 2. A) Study area Öschingen (view towards east, Photo: M. Danscheid); B) one example of a damaged building in Öschingen.

damage relates to general slope displacements, the open question is whether the damage results from shallow translational movements or from reactivations of the old large landslide blocks. Indeed, the expected size of landslide has major implications for mitigation measures.

3. Methodology

The study site in Öschingen was first investigated by detailed field inspection, including geomorphological analysis of the landslide complex. Based on the results,

drilling and inclinometer locations were chosen. Subsequently, the two geophysical methods (ground-penetrating radar (GPR) and 2D-resistivity (ERT)) were applied to achieve more comprehensive two-dimensional subsurface information:. The results of GPR and ERT investigations were then compared to drillings, penetration tests and inclinometer results.

3.1. Drillings, penetration tests and inclinometers

The aim of the drillings, penetration tests and inclinometers was to get information on the subsurface structure and dynamics of the whole landslide complex. Therefore, locations of investigations included the upper and lowest landslide blocks, the area above the damaged house and two more hummocky areas (Fig. 3). Six drillings were carried out using a drop-hammer and split-barrel samplers with liners. Locations and resulting depths are presented in Fig. 3. Drilling depths are the maximum depths which could be reached at the respective locations using the drop-hammer. Fourteen drop-penetration tests were performed with a weight of 50 kg and a drop height of 500 mm (Heavy Dynamic Penetration Test, DPH). The number of blows necessary to drive the penetration head (15 cm^2) 10 cm into the ground was counted and plotted on the graphs, showing penetration resistance in 10 cm increments.

In each of the six boreholes inclinometers were installed using plastic inclination tubes (55 mm diameter) and a portable measuring probe (NMG, System Glötzl) for step-by-step measurements in 50 cm units. The accuracy of the probe ranges between 0.01 and 0.1 mm for each measuring step, depending on the inclination angle of the tube, up to 5.5° and 30°, respectively. Analysis of the measurements was carried out using the software GLNP V3.1 (Glötzl). Measurements were carried out once a month after the inclinometers were installed (e.g. Oes1 (April 2004), Oes2 (April 2004), Oes6 (October 2004)).

3.2. 2D-resistivity (ERT)

At the Öschingen site, 2D-resistivity was the first choice for assessing subsurface data. Geoelectric measurements are conducted by applying a constant current into the ground through two current electrodes and measuring the resulting voltage differences at two potential electrodes. From the current and voltage values, an apparent resistivity value is calculated. 2D-surveys use 25 or more electrodes connected by a multi-core cable. To determine the subsurface resistivity in different zones or layers, an "inversion" of the measured apparent resistivity values (generally a total of some 100 single values) must be carried out. The result gives information on spatial averages of subsurface resistivities in a 2D-section. Basic details of the method are described by Loke and Barker (1995) or Kneisel (2003).

The main disadvantage of the ERT method is the wide range and the broad overlap of the possible subsurface resistivities of different geological units. Silty loam for example may show resistivities from 30 to 100 Ω m, while mudstone may range from 50 to $>10^5$ Ω m and limestone from 100 to 10^5 Ω m depending upon porosity and water content (Knödel et al., 1997, p. 92). Thus, resistivity changes due to varying moisture conditions may be by orders of magnitude higher than the differences between geological units. As a rule of thumb, weathered and partly disintegrated sliding masses usually stand out with a lower resistivity than the underlying bedrock (Bogolovsky and Ogilvy, 1977). However, in the current study area the atypical case of a resistivity increase in the sliding limestone blocks and a lower resistivity at the wet and clayey slip interface was expected.

The geoelectric measurements were carried out using a GeoTom unit (GeoLog2000, Augsburg/Germany) equipped with 50 electrodes. The electrode spacing was 4 m, which amounts to a total profile length of 196 m of each profile. The penetration depth was between 30 and 40 m (roughly 1/6 of the survey line). Four overlapping profiles were combined for a 500 m cross-profile along the lower slope terrace which is the lowest recognized landslide block. Two longitudinal profiles were measured perpendicularly to it (Fig. 3). A Wenner electrode configuration was used, which provides the best resolution for surface-parallel layers, but a comparatively weak accuracy for the detection of lateral inhomogenities (Knödel et al., 1997). The modelling of the resistivity distribution from the data was carried out using the Res2Dinv-software (Loke and Barker, 1995).

3.3. Ground-penetrating radar (GPR)

The principle of the GPR method is based on an electromagnetic pulse emitted from a transmitter antenna, reflected at inhomogenities and layer boundaries and received by a second antenna after a measured travel time. The whole array is moved along a profile line, which creates a 2D-section of the subsurface. Possible antenna frequencies range from 20 to 1000 MHz. A higher antenna frequency enhances the resolution of the data while lower frequencies increase the maximum penetration depth. A more detailed discussion of the GPR method can be found in Daniels (1996), Knödel et al. (1997) and Moorman et al. (2003).

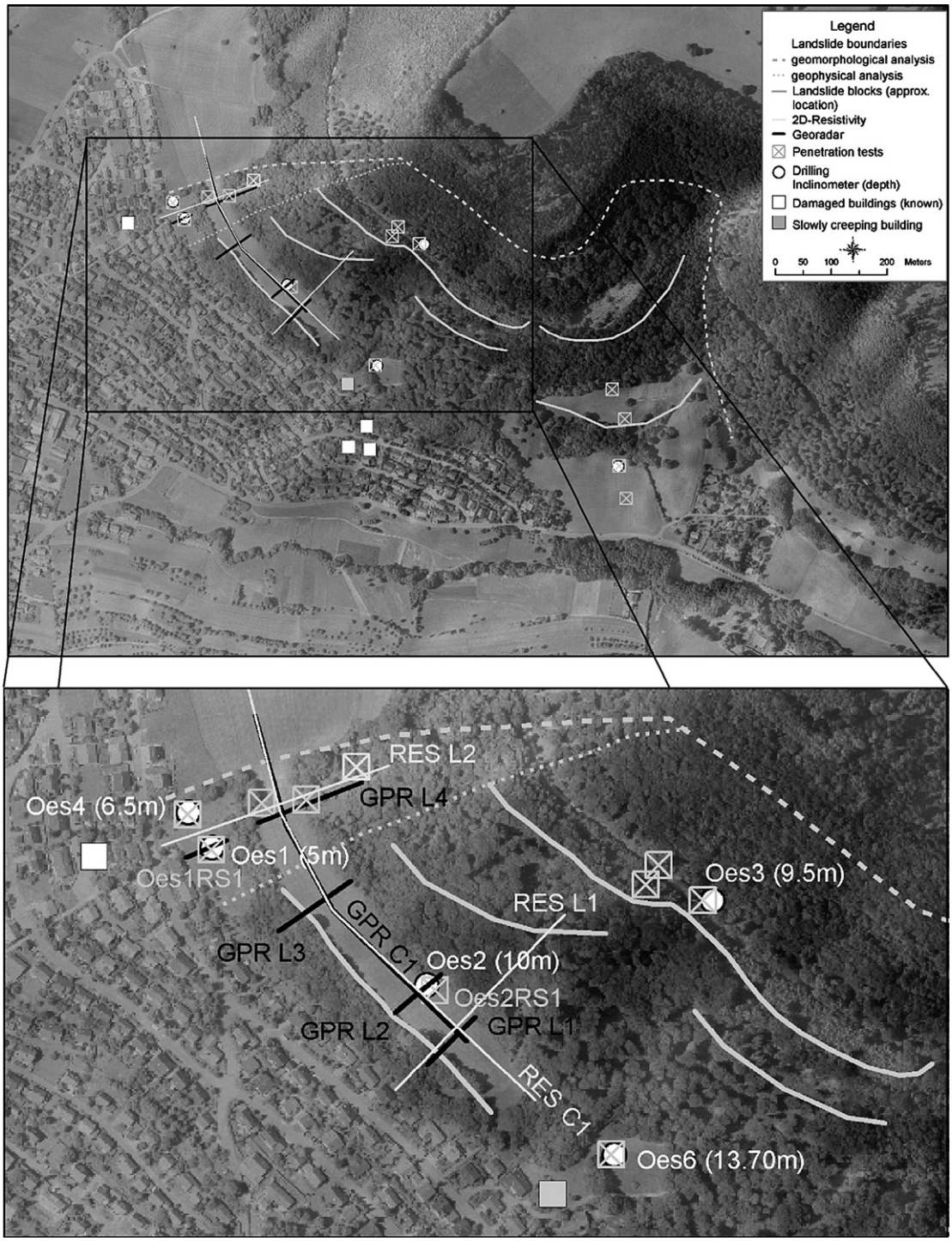

Fig. 3. Locations of investigations.

While geoelectrical measurements have become a common tool for subsurface exploration of landslides, GPR is very difficult to apply to landslide investigations. There are two major obstacles for the use of GPR in this environment. Firstly, the subsurface of landslides is usually wet and clayey which leads to a strong damping of the radar waves and to a limited penetration depth. Secondly, many landslides in humid temperate regions are more or

less densely covered with vegetation. This is also true for the Öschingen landslide. Forest near the profile line caused a very noisy dataset due to overhead reflections at the tree trunks when using unshielded antennas (shielded antennas were not available). Despite these limitations, it was tested if GPR can contribute subsurface information on the supposed limestone blocks.

A Ramac GPR device (Malå Geosystems, Sweden) equipped with 25, 50 and 100 MHz antennas was used. A long cross-profile was carried out across the lower slope terrace; four longitudinal profiles were measured perpendicular to it (see Fig. 3). The antenna separation was 4 m, 2 m and 1 m for the three antenna frequencies mentioned above. A trigger interval of 0.5 m was used with the 25 and 50 MHz antennas and of 0.25 m with the 100 MHz antennas. The specific velocity adaptation was achieved performing two WARR measurements (measuring with stepwise increasing antenna distance). The measured wave velocity was 0.075 m/ns which is typical for limestone debris with a high portion of silty loam. The vertical resolution (1/4 of the wavelength) was calculated to be 0.75 m (25 MHz), 0.38 m (50 MHz) and 0.18 m (100 MHz). The radargrams were processed using the ReflexW software (J. Sandmeier, Karlsruhe,

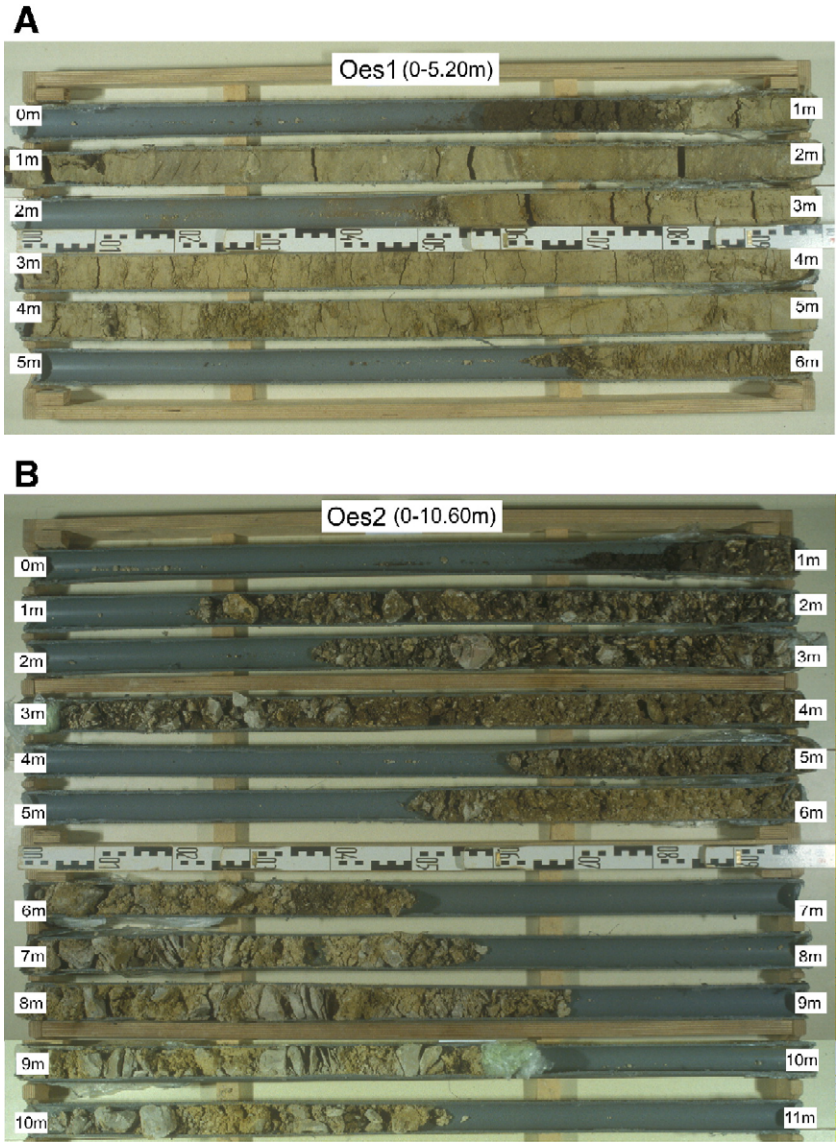

Fig. 4. View of the cores: A) Oes1 and B) Oes2 (refer to Fig. 3 for locations).

Germany). In most cases, a DC shift correction, a band pass filter, a static correction of the first onsets and a runtime-dependant gain function were applied.

4. Results and interpretation

4.1. Drillings, penetration tests and inclinometers

From the drilling cores two are selected which are next to the geophysical investigations. Core Oes2 shows crashed limestone blocks in a silty and clayey matrix (Fig. 4B). Whereas the lower parts (deeper than approximately 6 m) are part of the landslide block, the upper parts seem to be colluvium, which is reasonable since the drilling is located at a depression (Fig. 3). Unfortunately, the bedrock (middle Jurassic clay) and probably the sliding plane could not be reached. Core Oes1 contains only fine material, middle Jurassic clays with various degrees of weathering, indicating that this area may not be part of the old landslide (Fig. 4A).

The penetration test Oes1RS1 is in good agreement with the core Oes1 (Fig. 5). The increasing resistance with depth relates to the decreasing weathering state of the clays. Penetration test Oes2RS1 shows little variation, apart from some limestone blocks which had to be broken by the drop-hammer (Fig. 5). A boundary between colluvium and landslide block could not be found. At 11.20 m depth the tests had to be stopped due to the high resistance. Since the drilling stopped at 10.50 m, probably due to an unbreakable limestone block, it remains unclear whether the stop was caused by another large limestone block or by dry clay which could be a sign that the shear surface was crossed.

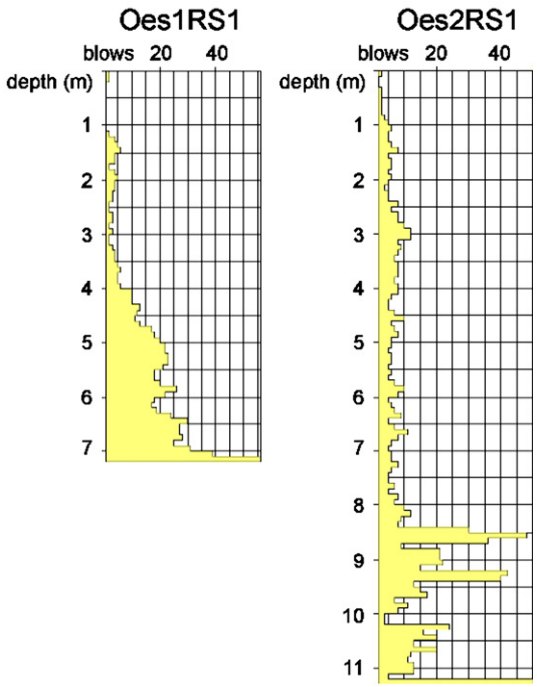

Fig. 5. Results of the penetration test Oes1RS1 and Oes2RS1 (refer to Fig. 3 for locations).

In general, all inclinometers showed very little movements if at all. No significant movements are indicated by the inclinometer Oes2 (Fig. 6B). However, since the inclinometer does not cross the sliding plane and thus, is not grounded in stable bedrock, there is the possibility that the whole landslide block may move slowly downwards together with the inclinometer without influencing the inclination. Although not presented here, similar results can be found for the inclinometer Oes3. Inclinometer Oes1 (Fig. 6A) shows no significant movement since April 2004, except some limited and shallow sliding following heavy snowmelt in March and April 2005. Some stronger and deeper movements are presented in the graph of inclinometer Oes6 (Fig. 6C), which is located outside the area of geophysical investigations. These movements also occurred after heavy snowmelt in Spring 2005.

4.2. Ground-penetrating radar (GPR)

The GPR results were affected by a strong attenuation of the radar waves. Thus, the penetration depth was restricted to 4 m (100 MHz), 6–8 m (50 MHz) and 8–13 m (25 MHz). The best results were obtained in the areas of high subsurface resistivity (see Section 4.3), while the highly conductive colluvium caused a stronger damping and made the results almost useless. Furthermore, the data analysis was severely disturbed by overhead reflections from the nearby woods above and below the terrace. The radiation characteristics of the dipole antennae include a higher portion of energy emitted parallel to the profile line than perpendicular to it (Daniels, 1996). According to this geometry, the disturbance of the longitudinal sections was more aggravating and prevented the detection of the base of the slide in these profiles. The overhead reflections of the forest at both ends of the profile are visible as two bunches of diagonal lines (Fig. 7). However, near-surface sediment structures were detected at profile GPR L1 with all the three frequencies utilised (25 and 50 MHz are presented in Fig. 7), which point to an antithetic rotation of the landslide block. The detected structures dip towards the slope in an angle of 10–15°. The block is separated from the slope above by a small depression filled with loamy sediments; its upper edge is visible as a reflector dipping steeply to the left. Similar structures were recognized in

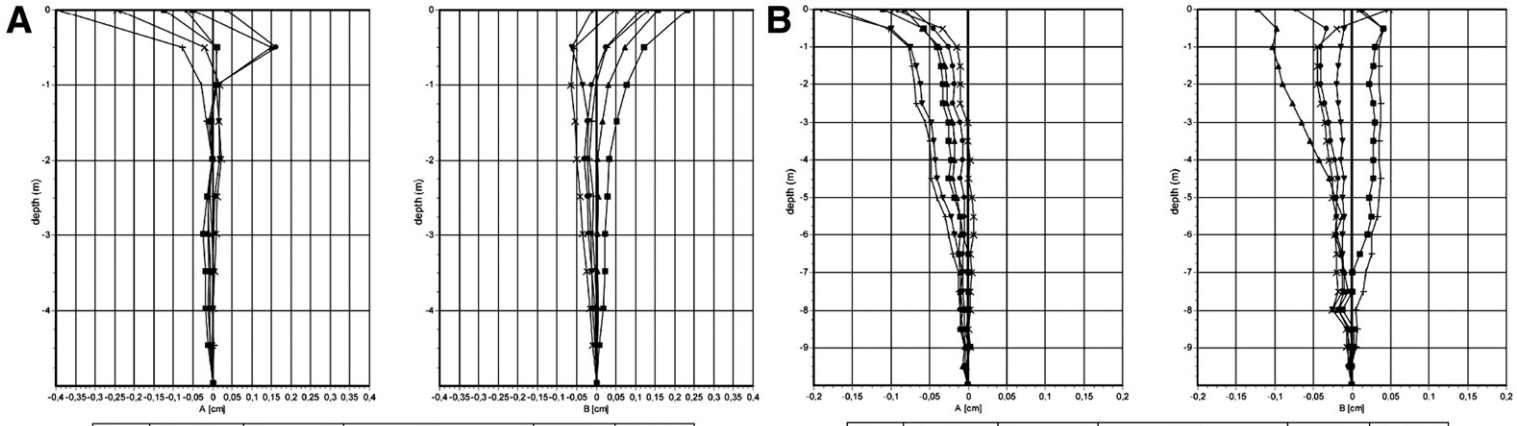

Line	Location	Measurements	Date	Diff. days	Depth (m)
●—	Oes01	28-00	17.05.2005-01.04.2004	411	5
▲—	Oes01	27-00	14.04.2005-01.04.2004	379	5
■—	Oes01	23-00	22.02.2005-01.04.2004	328	5
+—	Oes01	17-00	15.12.2004-01.04.2004	259	5
▼—	Oes01	09-00	13.09.2004-01.04.2004	166	5
×—	Oes01	04-00	14.07.2004-01.04.2004	105	5

Line	Location	Measurements	Date	Diff. days	Depth (m)
●—	Oes2	22-01	17.05.2005-13.05.2004	370	10
▲—	Oes2	21-01	14.04.2005-13.05.2004	337	10
■—	Oes2	17-01	21.01.2005-13.05.2004	254	10
+—	Oes2	15-01	06.01.2005-13.05.2004	239	10
▼—	Oes2	13-01	15.12.2004-13.05.2004	217	10
×—	Oes2	07-01	13.09.2004-13.05.2004	124	10

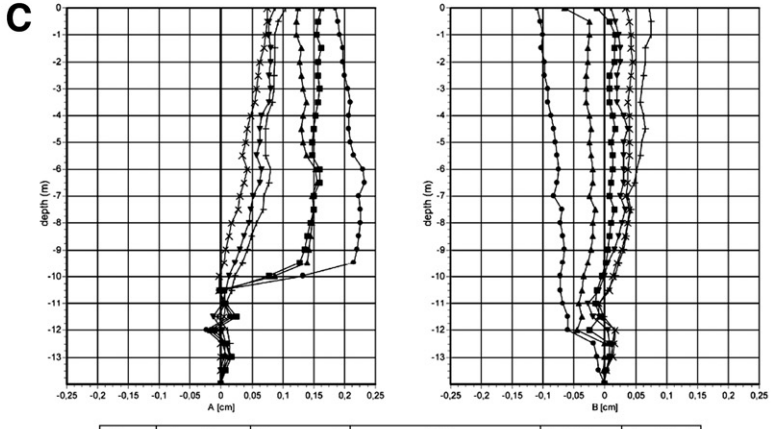

Line	Location	Measurements	Date	Diff. days	Depth (m)
●—	Oes6	16-02	17.05.2005-28.11.2004	170	14
▲—	Oes6	15-02	14.04.2005-28.11.2004	137	14
■—	Oes6	12-02	05.04.2005-28.11.2004	128	14
+—	Oes6	11-02	04.02.2005-28.11.2004	69	14
▼—	Oes6	09-02	21.01.2005-28.11.2004	55	14
×—	Oes6	06-02	05.01.2005-28.11.2004	38	14

Fig. 6. Results of inclinometer measurements of locations: A) Oes1, B) Oes2 and C) Oes6 (refer to Fig. 3 for locations). Note: The scale of the diagrams differs.

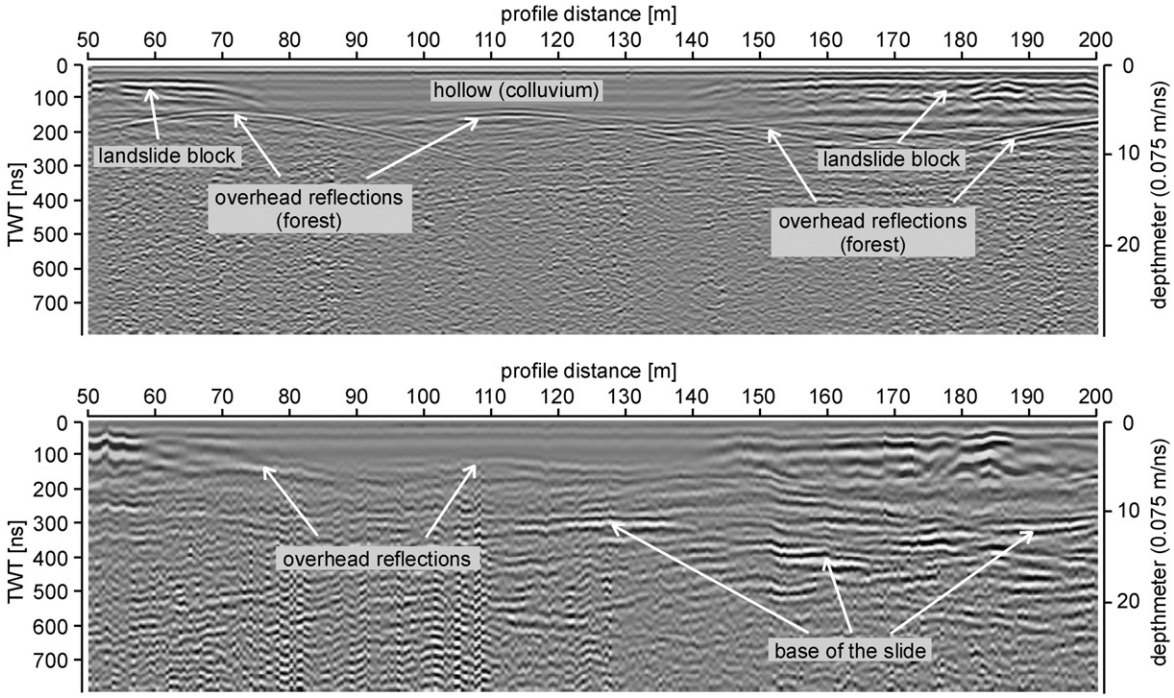

Fig. 7. Longitudinal profile GPR L1, 50 MHz (above) and 25 MHz (below).

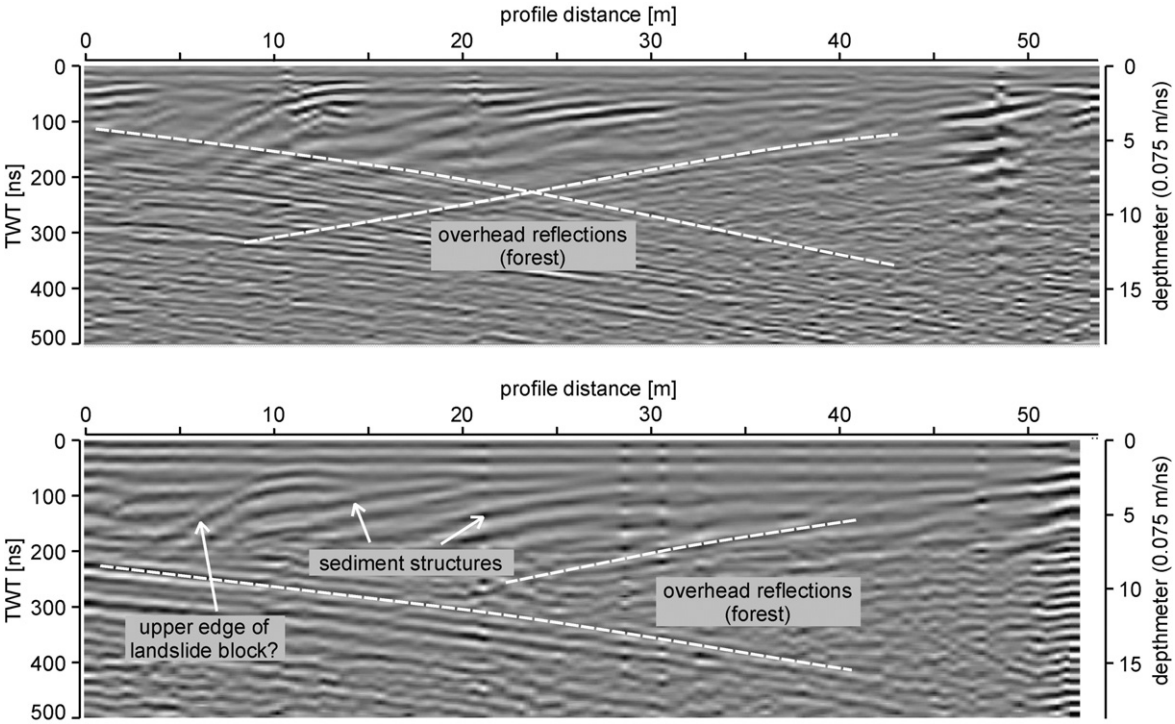

Fig. 8. Part of the GPR cross-profile, 50 MHz (above) and 25 MHz (below); right end is on longitudinal profile line L1.

longitudinal profile GPR L3, while GPR L2 and L4 provided almost no valuable information due to damping and overhead reflections.

The cross-profile rendered it possible to distinguish landslide blocks from colluvium due to the strong damping in the latter substrate (Fig. 8), which concurs with the nearby borehole information (Oes2). Two separated blocks were detected. Particularly in the 50 MHz profile, nearby trees became clearly visible as distinct reflection hyperbolae preventing the assessment of the deeper subsurface. Note the distinct hyperbolic reflections of trees in the 50 MHz profile; below, the subsurface information is covered by noise. Due to the larger wavelength, the forest reflections are less pronounced in the 25 MHz profile. Thus, the base of the slide is visible in part of this cross-profile as a bunch of roughly surface-parallel reflections. The depth of 11–12 m may support the hypothesis that, at least, the penetration test Oes2RS1 reached the shear plane.

4.3. 2D-resistivity (ERT)

The immanent error (RMS error) of the calculated inversion models ranged from 1.0 to 4.0% indicating good and reliable results. The only exception was one part of the cross-profile where contact problems between the cables and single electrodes probably led to noisier data and a higher RMS error in a small, restricted area of the cross-profile. These problems led to a slightly higher error of 6.3% but do not gravely affect the data interpretation.

The combined cross-section at the slope terrace clearly illustrates depth and lateral extent of the landslide (Fig. 9A). The displaced limestone blocks stand out with a much higher resistivity than the surrounding clayey sediments. Two large blocks can be marked out. The right (south-eastern) one reaches up to 15 m in thickness. Lower resistivity values in the upper parts point to advanced weathering and disintegration near the surface. The left one (middle of the profile) reaches a thickness of approximately 10 m. However, the ERT method is not suitable to derive exact depths because sharp boundaries tend to be smoothed especially in the lower parts of the profiles. Due to inaccuracies of the inversion process, a connection (or separation) of the blocks cannot be determined from the data. At any rate, the shallow depression at a profile distance of 340–360 m is obviously not the boundary between two landslide blocks.

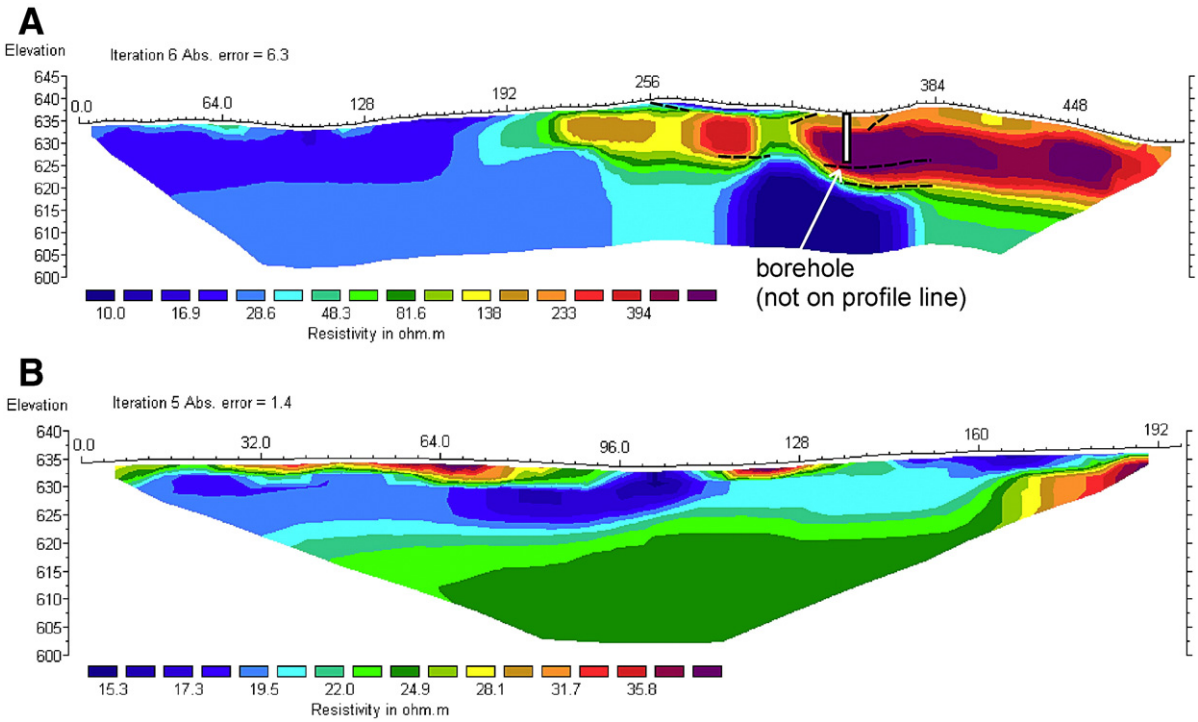

Fig. 9. 2D-geoelectrical profiles. A) Cross-section RES C1, combined from profiles RES C1a–RES C1d. Landslide area with displaced limestone blocks on the right side, undisturbed slope on the left side. Black dashed lines: georadar reflections. B) Cross-section RES C1d (left part of (a)), different contour values. C) Longitudinal section RES L1 (on the right of (a)). The inclinometer borehole is approximately 30 m north of the profile line. Black dashed lines: georadar reflections. D) Longitudinal section RES L2 (on the left of (a)). Black dashed line: georadar reflection.

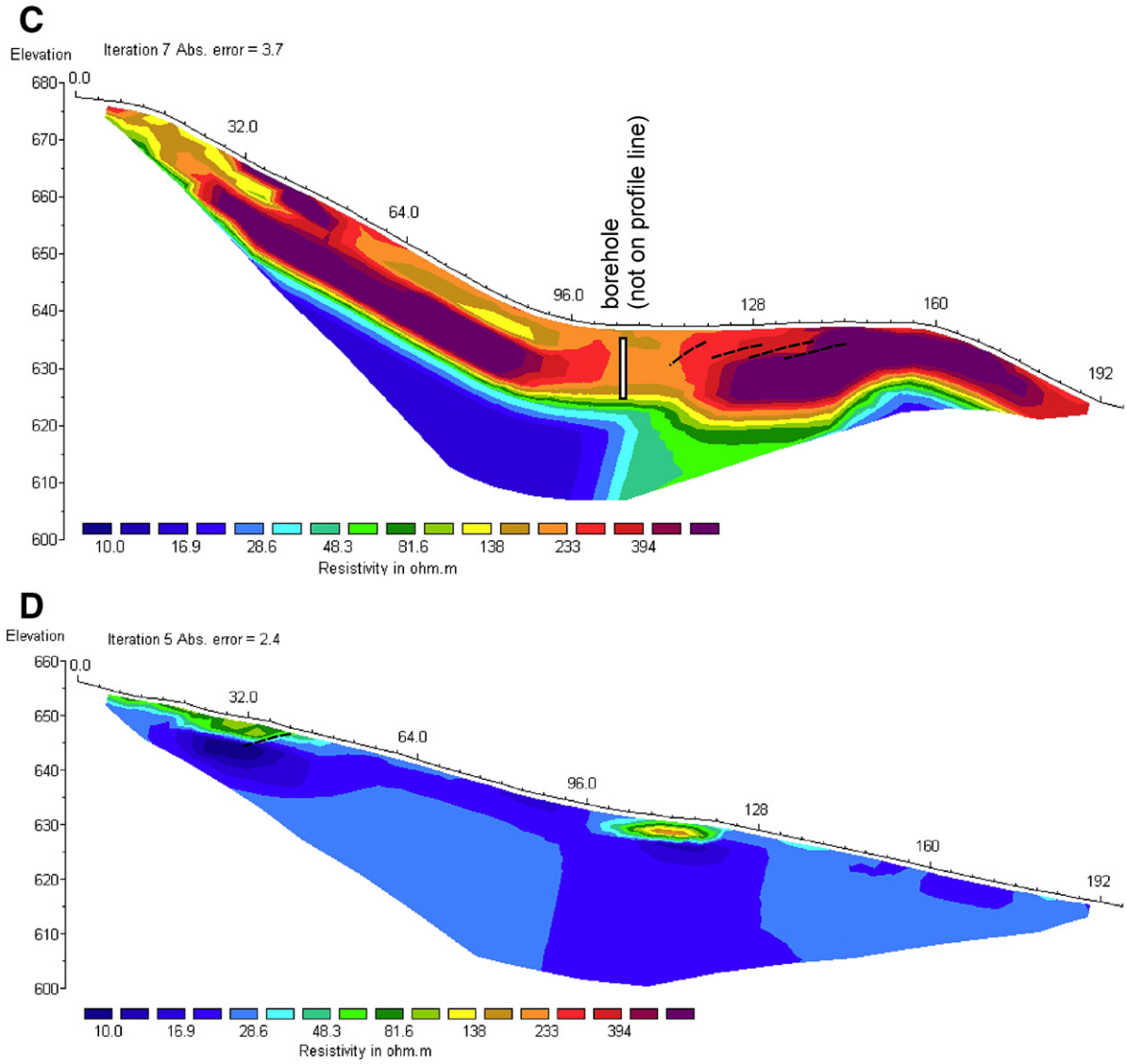

Fig. 9 (*continued*).

By contrast, the left (north-western) part of the cross-profile shows very low and rather uniform resistivity values with no evidence of landslide activity. The northernmost section is presented using a different colour chart in Fig. 9B. The enhanced conductivity in the uppermost 5–10 m may indicate the weathered colluvium overlying less weathered bedrock. The surface shows variations in resistivity probably due to different soil moisture conditions in very shallow ridges and depressions. Note that the absolute contrasts in resistivity are very low in this profile.

The results of the longitudinal profiles confirm the interpretation of the cross-profile. At the distinct terrace (profile RES L1, Fig. 9C) a very sharp boundary between displaced limestone blocks and underlying clayey bedrock can be recognized. The landslide material is divided into two areas of high resistivity. The position of the lower block coincides with the observed antithetic rotation structures of the GPR profile. The thickness is estimated to be 10–16 m. No outcrop of higher conductive middle Jurassic bedrock can be recognized at the surface; the zone of high resistivity extends downslope to the end of the profile which is right at the uppermost houses of Öschingen. The bedrock surface obviously follows the topography; note the distinct upbulge of the landslide block/bedrock interface at 150–160 m profile distance. The slope above the terrace is characterized by high resistivities as well. A zone of particularly low

conductance is at a depth of approximately 7–15 m below the surface, probably pointing to a limestone block overlain by better conductive limestone debris. The sharp boundary to the much higher conductive bedrock can be clearly recognized at a depth of 15 m.

The second longitudinal profile (Fig. 9D) confirms the absence of major sliding masses in this position. The profile is very uniform with the notable exception of two drier zones at the very surface. While the lower one coincides with a strip of woodland and bushes crossing the profile and probably leading to better drainage near the surface, the upper one corresponds with a small, superficial slide in this position. The slip surface is clearly indicated by lower resistivity (higher water content or higher portion of clays) and corresponds with a GPR reflection in the same position.

5. Conclusions

5.1. Suitability of the methods

The two very different geophysical techniques showed a rather good coincidence in detecting the base of the Öschingen landslide, which might be roughly supported by the penetration test. Surprisingly, ERT and GPR clearly detected the absence of large landslide blocks in the north-west, which could not be concluded from the geomorphology of this area. Following geomorphological investigations, the boundary of the landslide would have been delineated further to the north-west where the slope terrace ends. However, the results of the geophysical applications are supported by the drilling and penetration test.

Drillings and inclinometer measurements are still crucial to gain insight into structure and slip surfaces of a landslide and to validate any geophysical measurements. However, in the silty, comparatively wet and conductive substrate 2D-resistivity turned out to be the best choice to get detailed spatial information on thickness and extent of the slope movement. Landslide blocks were clearly distinguished from underlying bedrock and adjacent slope sediments. The data collection and processing was quick and effective which is partly due to the excellent interactive handling and survey speed of the GeoTom ERT equipment.

Gaining ground-penetrating radar information from deeper than 10 m was handicapped by the strong damping of loamy sediments and by overhead reflections in woody terrain. Thus, GPR will probably never be the first choice for landslide investigation when other geophysical methods are available. Despite these drawbacks, GPR provided valuable additional information on the near-surface structure of the landslide. Small-scale sediment structures like antithetic rotation of layers cannot be derived from any other geophysical technique. The detected bedrock surface under a part of the cross-profile helped validate the penetration test and ERT data. However, the outcome of the GPR measurements is limited compared to the 2D-resistivity sections.

5.2. Landslide structure and dynamics

The combination of geophysical and traditional techniques for subsurface exploration provided very valuable information on the Öschingen landslide structure. The sliding plane as well as the lateral boundary of the landslide could be detected. The latter could not be derived from geomorphological information alone. However, only a small part of the whole landslide complex was investigated. Further geophysical investigations will be carried out in the future to fully understand the structure of the landslide and to answer the question of the landslide type raised in the Introduction.

Regarding the current displacement rates, the inclinometer measurements show rather low landslide movement. Very slow and shallow translational movements occurred above the damaged house. Stronger and deeper movements were recognized in the hummocky areas. Keeping the limitations of the installed inclinometers in mind, the large landslide blocks seem to be dormant during the measured period. However, future tachymetric surveys will either validate these results or show that the landslide blocks are sliding without changing the inclination of the inclinometers. If financial resources become available deep drilling and a long inclinometer tube will give deeper insight into the dynamics of the lowest landslide block.

Based on these preliminary results it seems that beside very slow and shallow movements a catastrophic failure of the whole slope or parts of it is rather unlikely at present. However, further investigations (e.g. tachymetric surveying, slope stability analysis) and landslide monitoring (using inclinometer measurements) may lead to another conclusion in the near future, which then would have major implications for the treatment of the whole landslide complex by the local authorities.

Acknowledgements

We thank the German Research Foundation (DFG) for financial support of the project (GL 347/3). Special thanks go to the State Institute for Environmental Protection (LfU) and the Ministry of Environment and Transport Baden Württemberg for providing data. We

are grateful to Raphael Holland, Tanja Borchert, Christoph Kany, Nele Meyer, Maria Brennecke, Ruth Delzeit, Christina Schierlitz and Alejandro Garcia for their assistance. Furthermore we are indebted to the Institute of Geophysics in Stuttgart for hiring out the ERT equipment. Finally, we thank Alberto Corsini and an anonymous reviewer for improving the quality of the manuscript.

References

Agnesi, V., Camardo, M., Conoscenti, C., Dimaggio, C., Diliberto, I.S., Madonia, P., Rotigliano, E., 2005. A multidisciplinary approach to the evaluation of the mechanism that triggered the Cerda landslide (Sicily, Italy). Geomorphology 65, 101–116.

Bell, R., Kruse, J.-E., Garcia, A., Glade, T., Hördt, A., 2006. Subsurface investigations of landslides using geophysical methods — geoelectrical applications in the Swabian Alb (Germany). Geographica Helvetica 61, 201–208.

Bibus, E., 1986. Die Rutschung am Hirschkopf bei Mössingen (Schwäbische Alb). Geowissenschaftliche Rahmenbedingungen — Geoökologische Folgen. Geoökodynamik 7, 333–360.

Bibus, E., 1999. Vorzeitige, rezente und potentielle Massenbewegungen in SW-Deutschland — Synthese des Tübinger Beitrags zum MABIS-Projekt. In: Bibus, E., Terhorst, B. (Eds.), Angewandte Studien zu Massenbewegungen. Tübinger Geowissenschaftliche Arbeiten, Tübingen, pp. 1–58.

Bichler, A., Bobrowsky, P., Best, M.G., Douma, M., Hunter, J., Calvert, T., Burns, R., 2004. Three-dimensional mapping of a landslide using a multi-geophysical approach: the Quesnel Forks landslide. Landslides 1, 29–40.

Bogolovsky, V.A., Ogilvy, A.A., 1977. Geophysical methods for the investigation of landslides. Geophysics 42, 562–571.

Cruden, D.M., Varnes, D.J., 1996. Landslide types and processes. In: Turner, A.K., Schuster, R.L. (Eds.), Landslides: Investigation and Mitigation. National Academy Press, pp. 36–75.

Daniels, D.J., 1996. Surface-Penetrating Radar. Inst. of Electrical Engineers; Radar, Sonar, Navigation and Avionics Series 6, London. 300 pp.

Demoulin, A., Glade, T., 2004. Recent landslide activity in Manaihan, Belgium. Landslides 1, 305–310.

Dikau, R., Brunsden, D., Schrott, L., Ibsen, M. (Eds.), 1996. Landslide Recognition. Identification, movement and causes. Wiley, Chichester. 251 pp.

Fundinger, A., 2006. Ingenieurgeologische Untersuchung und geologische Kartierung (Dogger/Malm) der näheren Umgebung der Rutschungen am Hirschkopf bei Mössingen und am Irrenberg bei Thanheim (Baden-Württemberg). Diplomarbeit. Eberhard-Karls-Universität, Tübingen. 125 pp.

Glade, T., 2001. Landslide hazard assessment and historical landslide data — an inseparable couple? In: Glade, T., Frances, F., Albini, P. (Eds.), The Use of Historical Data in Natural Hazard Assessments. Kluwer, Dordrecht, pp. 153–168.

Glade, T., Stark, P., Dikau, R., 2005a. Determination of potential landslide shear plane depth using seismic refraction—a case study in Rheinhessen, Germany. Bulletin of Engineering Geology and Environment 64, 151–158.

Glade, T., Anderson, M.G., Crozier, M.J. (Eds.), 2005b. Landslide Hazard and Risk. Wiley, Chichester. 807 pp.

Godio, A., Bottino, G., 2001. Electrical and electromagnetic investigation for landslide characterisation. Physics and Chemistry of the Earth Part C: Solar–Terrestial and Planetary Science 26, 705–710.

Hecht, S., 2001. Anwendung refraktionsseismischer Methoden zur Erkundung des oberflächennahen Untergrundes. Stuttgarter Geographische Studien, vol. 131. Stuttgart. 165 pp.

Hecht, S., 2003. Differentiation of loose sediments with seismic refraction methods — potentials and limitations derived from case studies. Zeitschrift für Geomorphologie Neue Folge. Supplementband 132, 89–102.

Israil, M., Pachauri, A.K., 2003. Geophysical characterization of a landslide site in the Himalayan foothill region. Journal of Asian Earth Sciences 22, 253–263.

Kallinich, J., 1999. Verbreitung, Alter und geomorphologische Ursachen von Massenverlagerungen an der Schwäbischen Alb auf der Grundlage von Detail-und Übersichtskartierungen. Tübinger Geowissenschaftliche Arbeiten, Reihe D: Geoökologie und Quartärforschung, Tübingen. 166 pp.

Kneisel, C., 2003. Electrical resistivity tomography as a tool for geomorphological investigations — some case studies. Zeitschrift für Geomorphologie Neue Folge. Supplementband 132, 37–49.

Knödel, K., Krummel, H., Lange, G., 1997. Geophysik. Handbuch zur Erkundung des Untergrunds von Deponien und Altlasten. Bundesanstalt für Geowissenschaften und Rohstoffe, vol. 3. Springer, Berlin. 1063 pp.

Kreja, R., Terhorst, B., 2006. GIS-gestützte Ermittlung rutschungsgefährdeter Gebiete am Schönerger Kapf bei Öschingen. Die Erde 136, 397–414.

Loke, M.H., Barker, R.D., 1995. Least-squares deconvolution of apparent resistivity. Geophysics 60, 1682–1690.

Marcato, G., Mantovani, M., Pasuto, A., Silvano, S., Tagliavini, F., Zabuski, Zannoni, A., 2006. Site investigation and modelling at "La Maina" landslide (Carnian Alps, Italy). Natural Hazards and Earth System Sciences 6, 33–39.

Mauritsch, H.J., Seiberl, W., Arndt, R., Römer, A., Schneiderbauer, K., Sendlhofer, G.P., 2000. Geophysical investigations of large landslides in the Carnic region of southern Austria. Engineering Geology 56, 373–388.

McGuffey, V., Modeer, J., Victor, A., Turner, A.K., 1996. Subsurface exploration. In: Turner, A.K., Schuster, R.L. (Eds.), Landslides: Investigation and Mitigation. Special Report. National Academy Press, Washington, D.C., pp. 231–277.

Mikkelsen, P.E., 1996. Field instrumentation. In: Turner, A.K., Schuster, R.L. (Eds.), Landslides: Investigation and Mitigation. Special Report. National Academy Press, Washington, D.C., pp. 278–316.

Moorman, B.J., Robinson, S.D., Burgess, M.M., 2003. Imaging periglacial conditions with ground-penetrating radar. Permafrost and Periglacial Processes 14, 319–329.

Ortigao, J.A.R., 2004. Instrumentation. In: Ortigao, J.A.R., Sayao, A.S.F.J. (Eds.), Handbook of Slope Stabilisation. Springer, Berlin, pp. 425–465.

Schädel, K., Stober, I., 1988. Rezente Groβrutschungen an der Schwäbischen Alb. Jahreshefte des Geologischen Landesamtes Baden-Württemberg 30, 431–439.

Schmidt, M., 1994. Erläuterungen zu Blatt 7520 Mössingen, Geologischen Karte 1:25 000 von Baden-Württemberg. Geologisches Landsamt Baden-Württemberg, Freiburg. 185 pp.

Schneider, G., 1971. Seismizität und Seismotektonik der Schwäbischen Alb. Enke, Stuttgart. 79 pp.

Suzuki, K., Higashi, S., 2001. Groundwater flow after heavy rain in landslide-slope area from 2D-inversion of resistivity monitoring data. Geophysics 66, 733–743.

Terhorst, B., 1997. Formenschatz, Alter und Ursachenkomplexe von Massenverlagerungen an der schwäbischen Juraschichtstufe unter besonderer Berücksichtigung von Boden-und Deckschichtenentwicklung. Tübinger Geowissenschaftliche Arbeiten, Reihe D 2 (Tübingen, 212 pp.).

Wetzel, K.-F., Sass, O., von Restorff, C., 2006. Mass movement processes in unconsolidated Pleistocene sediments — a multi-method investigation at the "Hochgraben" (Jenbach / Upper Bavaria). Erdkunde 60, 246–260.